Available online at www.sciencedirect.com
SCIENCE DIRECT®
Applied Radiation and Isotopes 64 (2006) 508–519
Applied Radiation and Isotopes
www.elsevier.com/locate/apradiso

A theoretical model evaluating the angular distribution of luminescence emission in X-ray scintillating screens

I. Kandarakis[a,*], D. Cavouras[a], D. Nikolopoulos[a], A. Episkopakis[a], N. Kalivas[b], P. Liaparinos[c], I. Valais[a], G. Kagadis[c], K. Kourkoutas[d], I. Sianoudis[d], N. Dimitropoulos[e], C. Nomicos[f], G. Panayiotakis[c]

[a]*Department of Medical Instruments Technology, Technological Educational Institution (TEI) of Athens, Agiou Spyridonos, Aigaleo, 122 10 Athens, Greece*
[b]*Greek Atomic Energy Commission, P.O. Box 60092, 15310, Agia Paraskevi, Greece*
[c]*Department of Medical Physics, Medical School, University of Patras, 265 00 Patras, Greece*
[d]*Department of Physics, Chemistry and Materials Technology, Technological Educational Institution (TEI) of Athens, Ag. Spyridonos, Aigaleo, 122 10 Athens, Greece*
[e]*Medical Center "Euromedica" Alexandas, Athens, Greece*
[f]*Department of Electronics, Technological Educational Institution (TEI) of Athens, Ag. Spyridonos, Aigaleo, 122 10 Athens, Greece*

Received 19 June 2005; received in revised form 22 November 2005; accepted 22 November 2005

Abstract

The aim of this study was to examine the angular distribution of the light emitted from radiation-excited scintillators in medical imaging detectors. This distribution diverges from Lambert's cosine law and affects the light emission efficiency of scintillators, hence it also affects the dose burden to the patient. In the present study, the angular distribution was theoretically modeled and was used to fit experimental data on various scintillator materials. Results of calculations revealed that the angular distribution is more directional than that predicted by Lambert's law. Divergence from this law is more pronounced for high values of light attenuation coefficient and thick scintillator layers (screens). This type of divergence reduces light emission efficiency and hence it increases the incident X-ray flux required for a given level of image brightness.

Keywords: Scintillators; X-ray imaging; Luminescence; Angular distribution

1. Introduction

Most medical imaging systems (X-ray radiography and fluoroscopy, X-ray computed tomography, single photon emission tomography, positron emission tomography) are based on scintillator radiation detectors. Scintillators, often employed in the form of thin layers (scintillating screens, phosphor screens), are designed to absorb a large fraction of the incident radiation and convert it into light. The latter is collected by various optical sensors (radiographic films, photocathodes in image intensifiers or photomultipliers, photodiodes, CCDs, etc) (Besch, 1998; Wieczorek, 2001; Hell et al., 2000; van Eijk, 2002). However, depending on the detector design, significant light losses may occur at the scintillator–optical sensor interfaces. If light collection is insufficient, image quality may be significantly degraded. In addition in radiation detectors operated in energy integration mode (projection X-ray imaging), this fraction may indirectly affect the patient dose burden. Hence, it is of importance to estimate the fraction of scintillator light collected by the optical sensor. In many detector designs adopted in modern digital imaging systems (e.g. digital radiography using fiber optic tapers) the fraction of light arriving at the optical sensor is largely determined by the angular distribution of luminescence light emission (Maidment and Yaffe, 1995; Yu et al., 1997; Haak et al., 1997). In addition, the shape of the angular distribution affects the overall performance of an image detector,

*Corresponding author. Tel.: +30210 5385 387/5385 375; fax: +30210 5910 975.
E-mail address: kandarakis@teiath.gr (I. Kandarakis).

0969-8043/$ - see front matter © 2005 Elsevier Ltd. All rights reserved.
doi:10.1016/j.apradiso.2005.11.016

e.g. luminescence efficiency and detector sensitivity, spatial resolution, signal to noise ratio, etc. In most practical applications it is assumed that light emission follows closely the distribution of Lambertian light sources. The latter is a source having a uniform radiance (light energy flux per unit of solid angle) across its surface and emits uniformly in all directions (Matveev, 1985; Begunov et al., 1988; Zalewski, 1995). However, previous experimental data on the angular distribution of light emitted by granular or non-granular scintillating screens do not agree with this assumption (Giakoumakis and Miliotis, 1985; Giakoumakis and Nomicos, 1985; Haak et al., 1997).

In the present study, the angular distribution of light emission from scintillating screens was modeled as a function of screen thickness and intrinsic physical properties of the scintillator material. The model developed was used to fit experimental angular distribution data obtained for various traditional scintillator materials (Gd_2O_2S:Tb, ZnSCdS:Ag). Fitting allowed the determination of the values of optical attenuation coefficients and to predict the angular distribution of some new scintillator materials (Gd_2O_2S:Eu, Gd_2O_2S: Pr, Gd_2O_2S:Pr,Ce,F, $Y_3Al_5O_{12}$:Ce, $YAlO_3$:Ce, $YTaO_4$:Nb). Finally, the effect of the shape of angular distribution on the X-ray luminescence efficiency (XLE) was examined.

2. Method and materials

2.1. Model for angular distribution of light emission

In the present study, photometric rather than radiometric quantities were considered, (i.e. luminance and luminous intensity instead of radiance and radiant intensity). The scintillator was considered to be in the form of a layer (scintillating screen or phosphor screen) of thickness T, irradiated by a parallel X-ray beam. The layer was subdivided into elementary thin layers of thickness dt as depicted in Fig. 1. These elementary layers absorb X-ray energy and produce light photons. The surface of each elementary thin layer was assumed to emit light according to Lambert's cosine law (Matveev, 1985; Begunov et al., 1988; Zalewski, 1995). This law imposes that the luminous intensity $dI(\vartheta)$ produced by a thin layer at depth t and directed at an angle ϑ, with respect to the normal, is given as (Matveev, 1985; Begunov et al., 1988; Zalewski, 1995).

$$dI(\vartheta) = dI(0)\cos\vartheta, \tag{1}$$

where $dI(0)$ is the luminous intensity directed perpendicular with respect to the surface of the thin layer (Fig. 1). Luminous intensity was defined as $dI = d\Psi_\lambda/d\Omega$, where $d\Psi_\lambda$ is the luminous flux (light energy flux in W/m^2) emitted within a solid angle $d\Omega$. The light energy flux may be expressed in terms of the incident X-ray energy flux and the X-ray absorption and conversion properties of the scintillator, using the following expression (Ludwig, 1971; Kandarakis et al., 2003):

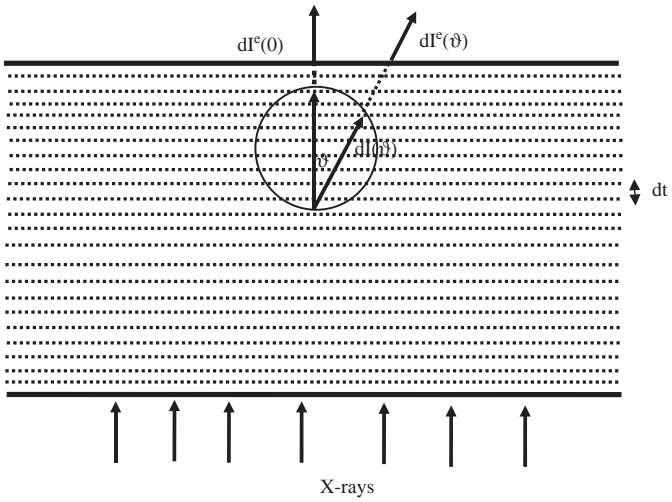

Fig. 1. Cross section of a scintillating screen subdivided in elementary thin layers. Depicted is the Lambertian emission of an elementary thin layer. $dI(\vartheta)$ is the luminous intensity produced by a thin layer dt at depth t and directed at an angle ϑ, $dI^e(\vartheta)$ is the corresponding luminous intensity emitted from the screen surface, $dI^e(0)$ is the luminous intensity emitted from the screen surface and directed perpendicular with respect to the surface.

$$d\Psi_\lambda = \int_0^{E_{max}} \bar{\psi}_x(E)\bar{\eta}(E,T)\eta_C x_R(E,t)\,dt\,dE, \tag{2}$$

where $\bar{\psi}_x(E)$ is the incident X-ray energy flux expressed in terms of spectral density (elementary flux per energy interval of the polychromatic X-ray spectrum) (Storm, 1972). E is the energy of an X-ray photon. $\bar{\eta}(E,T)$ is the X-ray energy absorption efficiency of the scintillating screen, i.e. the fraction of X-ray energy flux absorbed within scintillator mass. η_C is the X-ray to light conversion efficiency of the scintillator expressing the fraction of absorbed X-ray energy that is converted into light within the scintillator (Ludwig, 1971; Alig and Bloom, 1977; Blasse, 1994). $x_R(E,t)$ is a function giving the relative probability of X-ray absorption within an elementary thin layer of thickness dt, situated at depth t (see Appendix A). Integration is performed over the entire X-ray energy spectrum. E_{max} is the maximum energy of the X-ray spectrum which is numerically equal to the peak voltage applied to the X-ray tube. $\bar{\psi}_x(E)$ and $\bar{\eta}(E,T)$ express mean values of energy flux and absorption efficiency over the scintillating screen area.

As already mentioned $dI(\vartheta)$ expresses the luminous intensity generated within an elementary thin layer. However, due to light attenuation effects only a fraction of $dI(\vartheta)$ is transmitted through the rest of the screen towards a direction ϑ. This fraction may be expressed through the light transmission efficiency, $G(\vartheta,\sigma,t)$, describing the light attenuation effects within the screen mass. $G(\vartheta,\sigma,t)$ is given in terms of parameter σ (see Appendix A) (Swank,1973; Kandarakis and Cavouras, 2001), which is a function of the light absorption and light scattering

coefficients of the scintillator material. Thus, the luminous intensity emitted from the screen surface, denoted as $dI^e(\vartheta)$, is given by the relation

$$dI^e(\vartheta) = dI(\vartheta)G(\vartheta,\sigma,t) = [dI(0)\cos\vartheta]G(\vartheta,\sigma,t). \quad (3)$$

By taking into account relation (2) and the definition of luminous intensity ($dI = d\Psi_\lambda/d\Omega$), the fraction of light energy flux, created at depth t, which is emitted from the screen surface towards a direction ϑ may be written as follows:

$$dI^e(\vartheta)\,d\Omega = \int_0^{E_{max}} \bar{\psi}_x(E)\bar{\eta}(E,T)\eta_C x_R(E,t) \times \cos\vartheta G(\vartheta,\sigma,t)\,dt\,dE. \quad (4)$$

Finally, the total luminous intensity emitted by the whole screen towards ϑ may be obtained after integrating (4) over total screen thickness T:

$$I^e(\vartheta)\,d\Omega = \int_0^{E_{max}} \bar{\psi}_x(E)\bar{\eta}(E,T)\eta_C \int_0^T [x_R(E,t) \times \cos\vartheta G(\vartheta,\sigma,t)]\,dt\,dE. \quad (5)$$

As can be drawn out from Eq. (5), the angular distribution $I^e(\vartheta)$ of the emitted luminous intensity depends upon the product $\cos\vartheta G(\vartheta,\sigma,T)$. Thus, the angular distribution of $I^e(\vartheta)$ depends on the form and on the magnitude of the function $G(\vartheta,\sigma,t)$. This function is lower than unity and it decreases exponentially with distance (Swank, 1973). Hence, laterally directed light (at angles different than 90° with respect to the emitting screen surface) generated at every point within the scintillator mass is more significantly attenuated than light emitted at right angles (90° with respect to the emitting surface). This effect may cause a distortion of the shape of the angular distribution with respect to Lambert's cosine law. To examine the shape of the angular distribution and not its absolute values, the luminous intensity normalized to zero angle ($\vartheta = 0°$) was employed:

$$I^e_N(\vartheta) = I^e(\vartheta)/I^e(0). \quad (5b)$$

$I^e_N(\vartheta)$ is given in detail in the Appendix A (relation (A.5)).

To improve the accuracy of $I^e(\vartheta)$ calculations, the effect of K-fluorescence emission was also taken into consideration. Characteristic K-fluorescent X-rays may be generated in the scintillator material if the energy of the K-photoelectric absorption edge (K-shell) of one or more chemical elements in the material is encompassed by the incident X-ray beam spectrum. These K-fluorescent rays may be absorbed within the scintillator mass and create an additional site of light generation far from the site of primary X-ray absorption. This effect may distort the accurate registration of the spatial distribution of the incoming X-ray beam. Depending on the intensity of K-characteristic X-rays, image quality may be, more or less, degraded. On the other hand, if K X-rays escape the scintillator the intensity of emitted light is reduced. This influence of the K-fluorescence emission on the angular distribution of the emitted light was examined by employing a correction term $I^e_K(\vartheta)$. This term corresponds to the angular distribution of the light photons produced by the K X-rays absorbed in the scintillator. Since $I^e_K(\vartheta)$ refers to the additional light created by K X-rays, the final relation for the angular distribution may be given as follows:

$$I^e(\vartheta) = I^e_0(\vartheta) + I^e_K(\vartheta) \quad (5c)$$

$I^e_0(\vartheta)$ corresponds to the angular distribution in the absence of K-fluorescence emission.

2.2. Light signal loss and effect of angular distribution on XLE

The non-Lambertian shape of the angular distribution is expected to affect the total number of light photons emitted by a scintillating screen. Accordingly, the effect of angular distribution on scintillator's XLE was examined. XLE (η_λ), is defined as follows (Ludwig, 1971):

$$\eta_\lambda = \Psi^e_\lambda/\Psi_X, \quad (6)$$

where Ψ_X is the incident X-ray energy flux (total X-ray energy per unit of area and time). XLE is suitable for diagnostic radiology systems evaluation since the response of X-ray imaging detectors depends on the X-ray energy absorbed within the scintillator.

Eq. (5) gives the luminous flux $\Psi^e_\lambda(\vartheta)$ emitted by the scintillating screen within a solid angle element $d\Omega$. Considering that the light emission is azimuthally isotropic, $d\Omega = 2\pi\sin\vartheta\,d\vartheta$ and the total light energy flux emitted from the surface of the screen is written as

$$\Psi^e_\lambda = 2\pi\int_0^{\pi/2} I^e(\vartheta)\sin\vartheta\,d\vartheta, \quad (7)$$

$$\Psi^e_\lambda = 2\pi\int_0^{\pi/2} I^e(0)\sin\vartheta G(\vartheta,\sigma,t)\,d\vartheta \quad (7b)$$

or

$$\Psi^e_\lambda = 2\pi\int_0^{E_{max}} \bar{\psi}_x(E)\bar{\eta}(E,T)\int_0^{\pi/2}\int_0^T [x_R(E,t)\eta_C \times \cos\vartheta G(\vartheta,\sigma,t)]\,dt\,dE\,d\vartheta. \quad (7c)$$

If the angular distribution follows Lambert's cosine law, Eq. (1) can be taken into account and the light flux may be written as follows:

$$\Psi^e_{\lambda,L} = 2\pi\int_0^{\pi/2} I^e_L(0)\cos\vartheta\sin\vartheta\,d\vartheta. \quad (8)$$

The index L signifies that the corresponding luminous intensity and light energy flux follows a Lambertian distribution. $I^e_L(0)$ is the luminous intensity along the normal to the scintillator surface. Since $I^e_L(0)$ does not depend on ϑ, Eq. (8) leads to

$$\Psi^e_{\lambda,L} = 2\pi I^e_L(0)\int_0^{\pi/2}\cos\vartheta\sin\vartheta\,d\vartheta = \pi I^e_L(0). \quad (9)$$

To correct X-ray luminescence efficiency for the non-Lambertian distribution, Eq. (7) was first divided by Eq. (9). Thus the ratio ψ_λ of the actually emitted total energy flux over the total energy flux emitted by Lambertian surfaces is obtained. ψ_λ is often lower than unity and expresses the degree of optical signal loss due to deviation from Lambertian distribution. Considering the angular distribution normalized to $\vartheta = 0$ (i.e.$I^e_N(\vartheta) = I^e(\vartheta)/I^e(0)$) and assuming that $I^e(0) = I^e_L(0)$, it may be written as

$$\psi_\lambda = \frac{2}{I^e_L(0)} \int_0^{\pi/2} I^e(\vartheta) \sin\vartheta \, d\vartheta = 2 \int_0^{\pi/2} I^e_N(\vartheta) \sin\vartheta \, d\vartheta, \quad (10)$$

where$I^e_N(\vartheta)$ is a function of the angle ϑ and of the optical attenuation properties of the scintillator, expressed by the light transmission efficiency $G(\vartheta, \sigma, t)$. Thus, ψ_λ is also a function of $G(\vartheta, \sigma, t)$. X-ray luminescence efficiency may then be corrected as

$$\eta_\lambda = \eta_{\lambda L} \psi_\lambda, \quad (11)$$

where $\eta_{\lambda L}$ corresponds to the Lambertian distribution.

In a similar way the effect of non-Lambertian angular distribution on the detector optical quantum gain (OQG) may be determined. OQG is defined as the gain of a scintillating screen in number of quanta, i.e. the number of light photons emitted per one incident X-ray photon. This gain expresses the intensification effect of scintillating screens (intensifying radiographic screens) in medical radiography (Curry et al., 1990). OQG may be obtained by converting the X-ray energy flux and the light energy flux in X-ray photon and light photon flux. This may be done if the energy flux (Ψ) is divided by the energy of one photon (see Appendix A). Hence, η_λ may be converted into OQG if multiplied by the conversion factor $n(E, \lambda) = E/E_\lambda$, where E_λ is the mean energy of the emitted light photons and E is the energy of X-ray photons.

2.3. Measurements and calculations

The model Eqs. (5), (5b) and (A.5) (in Appendix A) were applied to fit experimental data obtained from measurements performed on Gd_2O_2S:Tb scintillating screens prepared in our laboratory. These equations were used to predict the normalized angular distribution of some new scintillator materials (Gd_2O_2S:Eu, Gd_2O_2S:Pr, Gd_2O_2S:Pr, Ce,F, $Y_3Al_5O_{12}$:Ce, $YAlO_3$:Ce, $YTaO_4$:Nb), which may be of particular interest for digital or conventional radiography and computed tomography. Europium (Eu) activated materials, like Gd_2O_2S:Eu, emit reddish light, which is very well compatible with photodiode and CCD arrays. Gd_2O_2S:Pr,Ce,F and Gd_2O_2S:Pr are considered suitable for X-ray computed tomography due to their high absorption efficiency and fast response. Cerium (Ce) activated scintillators (Gd_2O_2S:Pr,Ce,F, $Y_3Al_5O_{12}$:Ce, $YAlO_3$:Ce) are of interest in medical imaging due to their very short decay time (van Eijk, 2002). On the other hand $YTaO_4$:Nb has been previously shown to exhibit high image quality properties (Beutel et al., 1993). In addition, in order to investigate the effect of angular distribution shape on XLE, experimental data on both Gd_2O_2S:Tb, and ZnSCdS:Ag were employed. These data were derived from a previous study (Cavouras et al., 1999).

The scintillator materials were supplied in powder form by Derby Luminescent Ltd., Lumilux Ltd and Phosphor Technology Ltd. Screens of various thicknesses were prepared using sedimentation techniques (Diakides, 1973; Kandarakis et al., 1997). X-ray excitation was performed on a Philips Optimus radiographic unit incorporating a tungsten target X-ray tube. Various X-ray tube voltages ranging from 40 to 140 kVp were employed. Experimental techniques are described in detail in previous studies (Giakoumakis and Miliotis, 1985; Giakoumakis and Nomicos, 1985). The experimental setup comprised an EMI 9592 B photomultiplier equipped with an S-10 photocathode coupled to a Cary 401 electrometer with angular translation on a Rigaku-Denki SG-9D horizontal goniometer equipped with a 0.05° accuracy step scan controller.

Fitting was performed by the Levenberg–Marquard method (Press et al., 1990). Data on X-ray absorption properties of the scintillator materials and parameters related to their K-fluorescence emission effects were obtained from the literature (Storm and Israel, 1967; Hubbell and Seltzer, 1995; Hubbell et al., 1997). The function $\bar{\psi}_x(E)$ in (4), (5) and (A.5) expressing the X-ray spectral density was calculated according the theoretical model of Storm (Storm, 1972).

The function $\bar{\eta}(E, T)$, in (2), (5) and (A.5), was calculated using the following relation (Chan and Doi, 1983):

$$\eta(E, T) = (\mu_{tot,en}(E)/\mu_{tot,t}(E)) \times [1 - \exp(-\mu_{tot,t}(E)T], \quad (12)$$

where $\mu_{tot,t}(E)$ is the total mass X-ray attenuation coefficient at energy E, while $\mu_{tot,en}(E)$ is the corresponding total mass X-ray energy absorption coefficient (Storm and Israel, 1967; Hubbell and Seltzer, 1995). The latter expresses all modes of energy absorption i.e. energy transfer from primary X-rays to secondary electrons. However, $\mu_{tot,en}(E)$ has been defined by assuming that all energy transferred to secondary photons (e.g. K-fluorescence X-rays) escapes the absorbing material (Hubbell et al., 1997). Hence, the energy absorption efficiency, as calculated by relation (12), includes only the fraction of X-ray energy absorbed locally at the point of primary X-ray interaction. The effect of generation and re-absorption of K-fluorescent characteristic X-rays is not taken into account in relations (2), (5). To account for this effect the probability of generation and re-absorption of K-fluorescent X-rays was separately calculated as shown in the Appendix A (relations (A.8)–(A.12)). Then, by replacing $\bar{\eta}(E, T)$ (relations (2), (5)) with this probability, the

contribution, $I_K^e(\vartheta)$, of the K-fluorescent X-rays to the final angular distribution of emitted light was determined.

The intrinsic conversion efficiency, η_C in relations (4), (5), was used as a fitted parameter. However, an initial value of η_C was estimated by the relation

$$\eta_C = (h\nu/\beta E_G)Sq, \tag{13}$$

where ν is the mean frequency of the emitted light, E_G is the value of the forbidden band gap between the valence and the conduction energy bands of the scintillator material. β is a unitless parameter characterizing the excess energy, above E_G, required for electron–hole pair creation. S, q are transfer and quantum efficiencies related to the fraction of electron–hole pair energy, which is transferred to the activator and thus converted into light. In the present study S, q were initially taken to be equal to unity. In cases where data on E_G were not available η_C initial values were taken from previous studies (Alig and Bloom, 1977; Blasse, 1994).

The function $G(\vartheta, \sigma, t)$ describing the light transmission efficiency was modeled according to the radiative transfer theory as simplified by Swank's approximation to the diffusion equation (Swank, 1973). In this model, light attenuation effects (scattering and absorption) are expressed through two optical coefficients: the reciprocal optical diffusion length (σ) and the reciprocal optical relaxation length (τ). For details on these coefficients and on the model used, the reader is referred to previous studies (Ludwig, 1971; Swank, 1973; Kandarakis and Cavouras, 2001). Initial values for the light attenuation coefficients (σ, τ) were taken from previous studies (Kandarakis et al., 1997; Cavouras et al., 1999; Kandarakis and Cavouras, 2001).

Fitting was refined by allowing η_C, σ and τ to vary slightly from their initial values. For some of the new scintillator materials (Gd_2O_2S:Eu, Gd_2O_2S:Pr, Gd_2O_2S:Pr,-Ce,F, $Y_3Al_5O_{12}$:Ce, $YAlO_3$:Ce, $YTaO_4$:Nb) where optical data were not available, σ and τ were estimated by taking into account the dependence of these coefficients on light wavelength λ. This dependence was previously found (Kandarakis et al., 2005) to be of the form

$$\sigma = a + b \times (\bar{\lambda})^{-1} + c \times (\bar{\lambda})^{-2}, \tag{14}$$

where a, b, c are fitted parameters and $\bar{\lambda}$ is the mean wavelength of the light emission spectra of the scintillator materials. These spectra were either measured in our laboratory (Gd_2O_2S:Eu, Gd_2O_2S: Pr, Gd_2O_2S:Pr,Ce,F, $Y_3Al_5O_{12}$:Ce, $YAlO_3$:Ce) using an Oriel 7240 grating monochromator or taken from the literature ($YTaO_4$:Nb) (Curry et al., 1990; Blasse, 1994; Miura, 1999). This dependence of σ on wavelength is in accordance with what was expected from the well-known light absorption and light scattering laws, which state that light attenuation increases with decreasing wavelength (Van de Hulst, 1957).

3. Results and discussion

Fig. 2 shows curves of normalized angular distribution of light emission ($I_N^e(\vartheta) = I^e(\vartheta)/I^e(0)$ given by Eqs. (5b), (5) and (A.5) in Appendix A). These curves correspond to best fitting of the ratio $I_N^e(\vartheta) = I^e(\vartheta)/I^e(0)$ to experimental data. An additional curve corresponding to a normalized Lambertian angular distribution ($I^e(\vartheta)/I^e(0) = \cos\vartheta$) is also shown for comparison purposes. The curves presented were obtained from experimental data on Gd_2O_2S:Tb

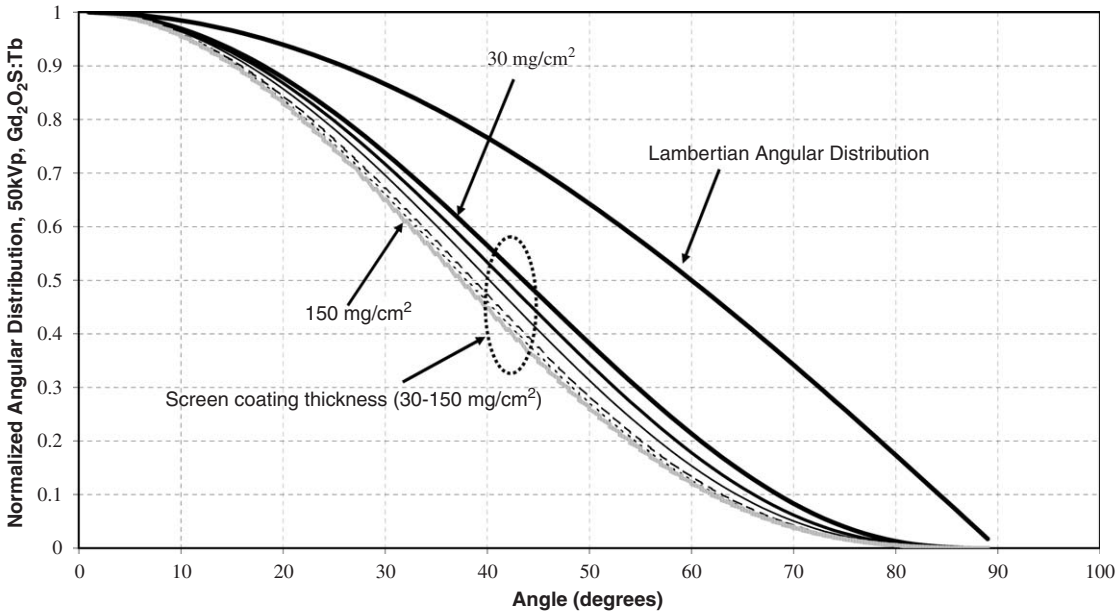

Fig. 2. Fitted curves of normalized angular distribution of light emitted by granular scintillating screens (Gd_2O_2S:Tb) of various coating thicknesses (30–150 mg/cm^2) at 50 kVp X-ray tube voltage. A curve corresponding to Lambertian distribution is also shown for comparison.

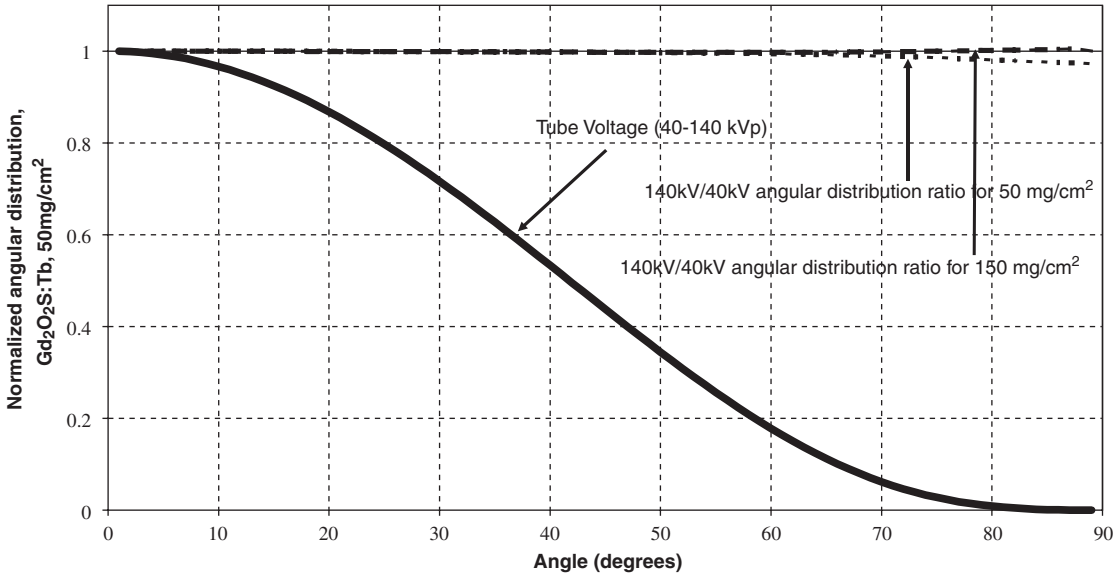

Fig. 3. Calculated curves of normalized angular distribution of light emitted by a granular scintillating screen (50 mg/cm^2) at various X-ray tube voltages.

scintillating screens of various coating thickness, from 30 to 150 mg/cm^2. Similar curves were obtained for the other scintillating materials and are not presented for brevity. As it may be observed: (i) the shape of the Lambertian curve differs clearly from the shape of the fitted curves, the latter being more directional (lower values at angles ϑ larger than 0°), (ii) screen coating thickness affects the shape of the light emission angular distribution. Thick screens exhibit lower normalized luminous intensity values in the range from $\vartheta = 20°$ to 70°. For the 150 mg/cm^2 screen, a 30% decrease in relative values was observed at $\vartheta = 50°$. This results in a more directional angular distribution shape, with respect to the corresponding Lambertian distribution, as screen thickness increases. Increased directionality of light emission may improve light collection by the optical sensor of the X-ray detector and ameliorate image quality (spatial resolution). In absolute luminous intensity values however, this directionality accounts for a fractional loss in absolute optical signal level (see ψ_λ in Eq. (10)). Therefore, it results in a relative decrease of X-ray luminescence efficiency (with respect to Lambertian screens). To provide a more physical explanation of this loss, the increasing amount of optical scattering, combined with absorption effects, has to be taken into consideration. Multiple scattering effects increase the total distance traveled by light photons within the additional thin scintillator layer (Δt), accumulated in thick screens. This in turn increases the probability of absorption and final extinction of light photons. Such effects are more pronounced for laterally directed photons, which are thus highly attenuated. To investigate the effect of varying X-ray tube voltage on the shape of the light angular distribution, angular distribution data for the same Gd_2O_2S: Tb scintillating screen (50 mg/cm^2) at various X-ray tube voltages were calculated and plotted (Fig. 3). As observed, all curves were found practically identical, being in almost perfect coincidence. This finding indicates that X-ray tube voltage (and X-ray energy) variation does not significantly affect the shape of the normalized angular distribution. Additional curves corresponding to the ratio of the angular distribution at 140 kVp over the angular distribution at 40 kVp, for two screens of 50 and 150 mg/cm^2, are also plotted in Fig. 3. To good approximation, the ratio remains constant over the whole range of angles thus confirming that X-ray tube voltage does not apparently affect angular distribution shape for both thin and thick screens. The effect of K-fluorescence X-ray production was also found to be of very low significance for the normalized angular distribution. Calculated data on this effect are shown in Fig. 4. This figure is a plot of the ratio $(I^e_{0,N}(\vartheta)/(I^e_{0,N}(\vartheta) + I^e_{K,N}(\vartheta))$ i.e. the normalized angular distribution values without correction for the K-fluorescence effects over the normalized angular distribution values corrected for the K-fluorescence effects. This ratio remains fairly constant in a range of angles up to $\vartheta = 60°$ indicating the low significance of these effects. This may be explained by considering the following: after primary X-ray photons interaction at a point within scintillator mass, K-fluorescence X-ray photons are isotropicaly created towards all directions. It may then be assumed that this property induces a, more or less, uniform spatial redistribution of X-ray photon interaction points within screen mass. This redistribution may significantly reduce the spatial accuracy of primary incident photon registration and may degrade image quality (spatial resolution, contrast). However, it seems that the shape of the angular distribution is not significantly distorted, at least to the degree of this redistribution being somewhat uniform. This is because a K X-ray absorption has no influence on the mechanisms of light creation and angular distribution shape determination,

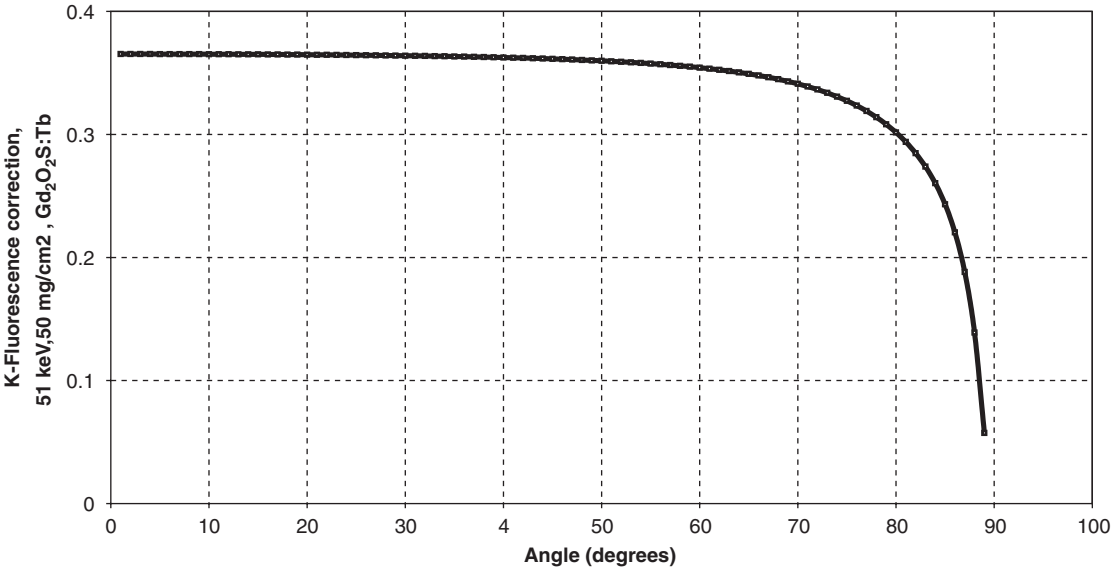

Fig. 4. Calculated ratio $(I^e_{0,N}(\vartheta)/(I^e_{0,N}(\vartheta)+I^e_{K,N}(\vartheta))$ of the normalized angular distribution values without correction for the K-fluorescence effects over the normalized angular distribution values corrected for the K-fluorescence effects. Data were calculated for 51 keV monoenergetic X-rays.

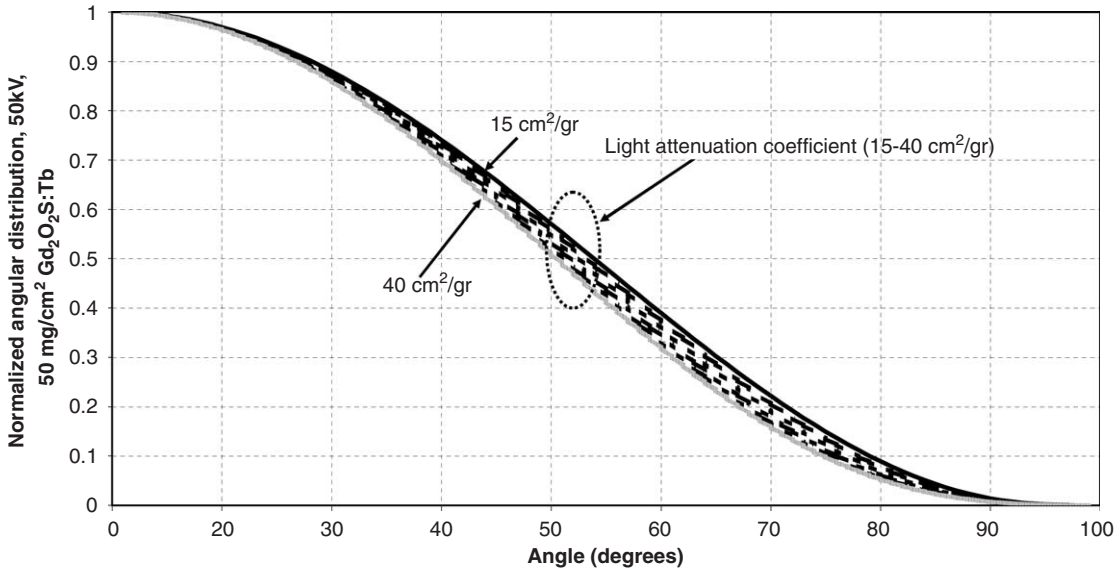

Fig. 5. Calculated normalized angular distribution of light emitted corresponding to Gd_2O_2S host material considering various values of the light attenuation coefficient σ.

i.e. Lambertian light emission from the elementary thin layers Δt and significant optical scattering when light is transmitted through the additional thin scintillator layers before final emission from screen surface.

Fig. 5 shows calculated normalized angular distribution curves obtained for the same host material (e.g. Gd_2O_2S) but for different values of the light attenuation coefficient σ. The shape of the angular distribution becomes more directional with increasing light attenuation coefficient. At $\vartheta = 45^\circ$ the difference between the upper curve, corresponding to $\sigma = 15\,cm^2/g$, and the lower curve, corresponding to $\sigma = 40\,cm^2/g$, was approximately 10%. For a given scintillator material host, e.g. Gd_2O_2S, and equal powder grain size, the light attenuation coefficient is affected by the emitted light spectrum of the scintillator (relation (14)), e.g. values in the range $\sigma = 20-25\,cm^2/g$ correspond to reddish light emission, while values in the range $\sigma = 30-35\,cm^2/g$ correspond to green or blue emission (Kandarakis et al., 1997; Kandarakis and Cavouras, 2001). The emitted spectrum is highly affected by the type of ion activator (e.g. Tb^{3+}, Eu^{3+}, Ce^{3+}, Ag, etc.) incorporated within the host material. A high efficiency scintillator host material (like Gd_2O_2S) may be employed with different activators in order to: (i) suitably

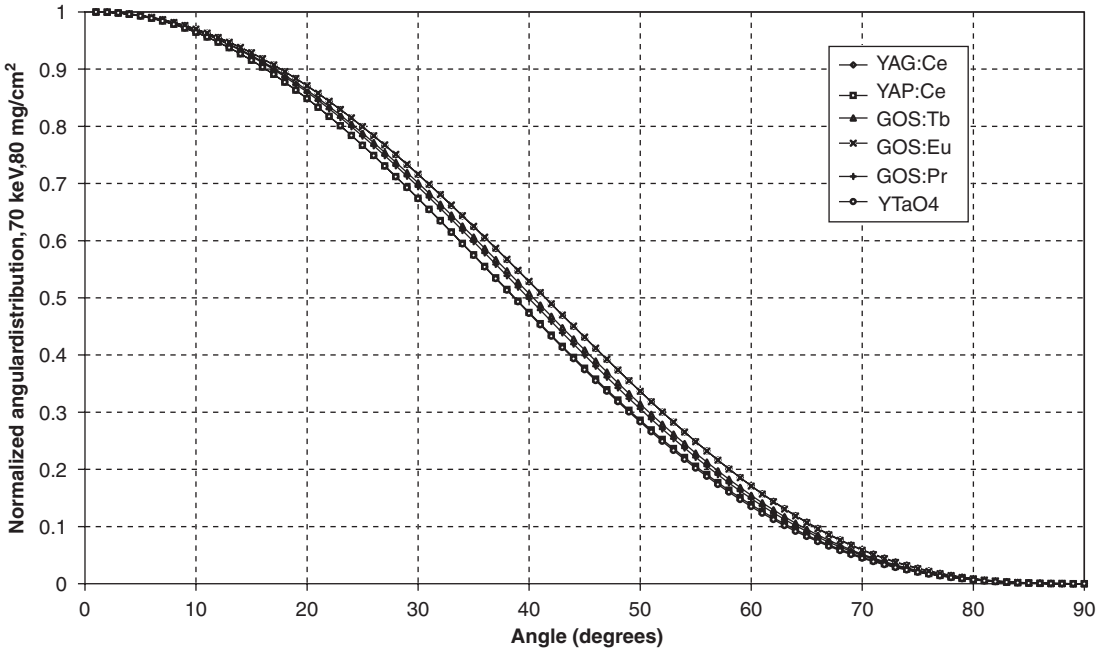

Fig. 6. Calculated curves of normalized angular distribution for various scintillator materials (Gd_2O_2S:Eu, Gd_2O_2S:Pr, Gd_2O_2S:Pr,Ce,F, $Y_3Al_5O_{12}$:Ce, $YAlO_3$:Ce, $YTaO_4$:Nb). Curves corresponding to Gd_2O_2S:Pr and Gd_2O_2S:Pr,Ce,F were found practically identical and were not separated.

Table 1
Intrinsic physical properties of scintillator materials

Scintillator	$\bar{\lambda}$ (nm)	σ (cm^2/g)	τ (cm^2/g)	η_C
Gd_2O_2S:Tb	545	30	1000	0.20
Gd_2O_2S:Eu	627	23.5	783	0.12
Gd_2O_2S: Pr	513	29	967	0.13
Gd_2O_2S:Pr,Ce,F	513	29	967	0.13
$Y_3Al_5O_{12}$:Ce	550	26	867	0.046
$YAlO_3$:Ce,	370	60	2000	0.056
$YTaO_4$:Nb	410	50	1667	0.11
ZnSCdS:Ag	550	33	1100	0.22

$\bar{\lambda}$ is the mean wavelength of the emitted light spectrum.

modify its emission spectrum to match the spectral sensitivity of different optical sensors incorporated in various detectors (e.g. change from Tb to Eu activator), (ii) ameliorate the decay time characteristics of the scintillator material (e.g. Ce activator), (iii) to modify the intrinsic conversion efficiency of the scintillator (Alig and Bloom, 1977; Blasse, 1994; van Eijk, 2002). However, as it may be deduced from data shown in Fig. 5, in all these cases the angular distribution may be altered and correspondingly the light collection efficiency and the overall detector efficiency may correspondingly be affected.

Fig. 6 shows calculated normalized angular distribution curves of various powder scintillator materials (Gd_2O_2S:Eu, Gd_2O_2S:Pr,Ce,F, $Y_3Al_5O_{12}$:Ce, $YAlO_3$:Ce, $YTaO_4$:Nb). 50 keV mono-energetic X-rays and 80 mg/cm^2 screen coating thickness were considered. Data corresponding to the intrinsic conversion efficiency, the mean emitted wavelength and the optical attenuation coefficients of these materials are shown in Table 1. As may be seen, all curves are very close, exhibiting very slight differences. At 45° the difference between highest (Gd_2O_2S:Eu) and lowest ($YTaO_4$) values were of the order of 5%. Gd_2O_2S: Eu has lower coefficient σ (15 cm^2/g) than $YTaO_4$ (40 cm^2/g). These results are in agreement with data plotted in Fig. 5. Scintillator materials with high light attenuation properties (e.g. $YTaO_4$: Nb, $YAlO_3$: Ce), corresponding to high values of coefficient σ, resulted in more directional angular distribution curves.

Fig. 7 shows calculated results on the variation of XLE with coating thickness considering Lambertian and non-Lambertian angular distribution. XLE is given in unitless values. Calculations were performed for 80-kVp X-ray tube voltage. Transmission mode or front screen configuration data are shown in both figures, i.e. light flux emitted from the non-irradiated side. This configuration corresponds to most scintillator–optical sensor combinations: digital radiology detectors, front screen in radiographic cassettes, etc. Values corresponding to non-Lambertian distribution were found to be significantly lower with respect to values from Lambertian one. The difference was found to vary from approximately 15% to 30% depending on scintillator material and screen coating thickness. Of very similar shape are the curves shown in Fig. 8. These curves represent calculated data on the OQG considering Lambertian and non-Lambertian angular distribution. Differences were of the order of 20–30% depending on screen coating thickness and scintillator material.

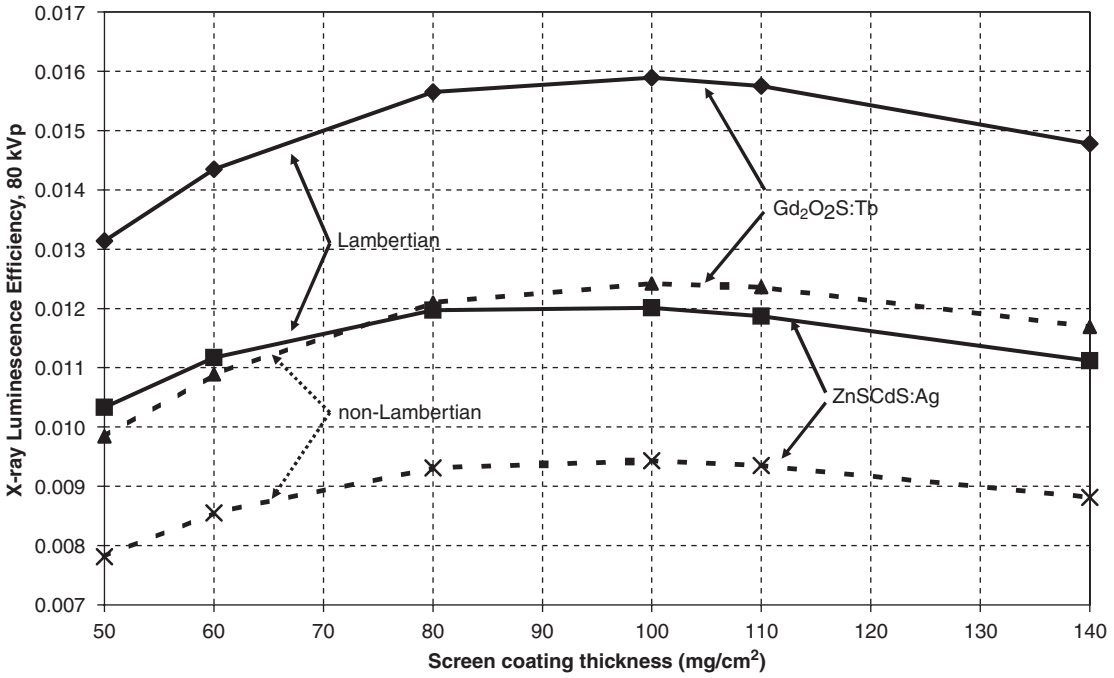

Fig. 7. Variation of X-ray luminescence efficiency with scintillator coating thickness for Lambertian and non-Lambertian distribution.

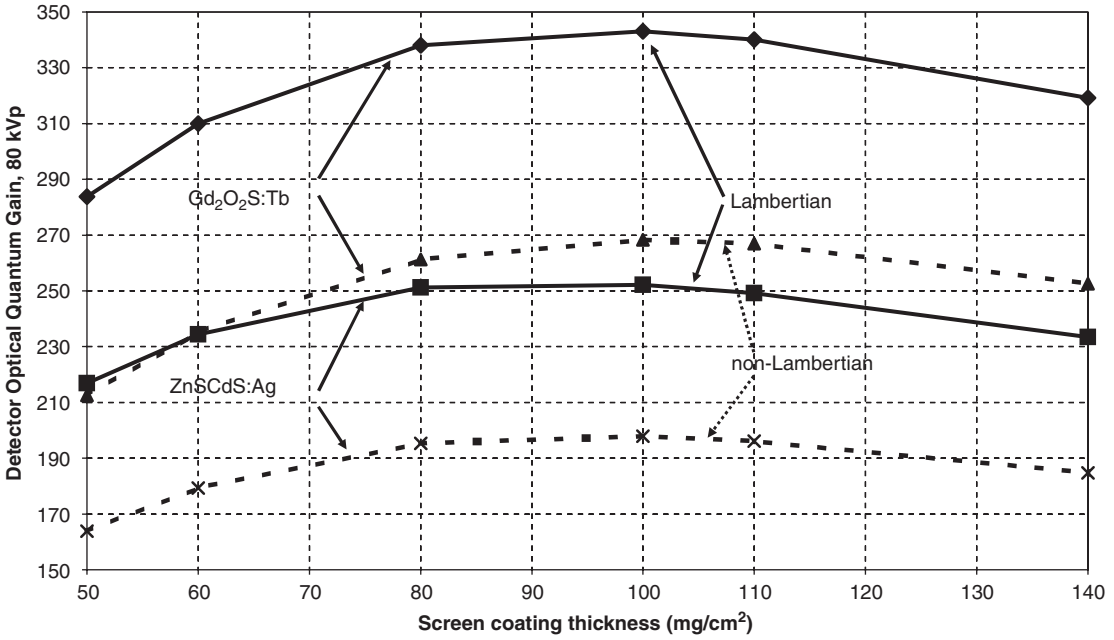

Fig. 8. Variation of optical quantum gain with scintillator coating thickness for Lambertian and non-Lambertian distribution.

4. Summary and conclusions

Model and data presented in this study indicate that the angular distribution of the light emitted by granular scintillators shows a divergence from the well-known Lambertian distribution. This divergence is mainly determined by the light attenuation properties of the scintillator materials, expressed by the combined effects of light scattering and absorption (light transmission efficiency). Scintillator light emission shows higher directionality than Lambertian sources, this directionality being more pronounced with increasing light attenuation coefficient. This effect may improve light collection by the optical sensor and ameliorate image quality. However, X-ray luminescence efficiency and optical quantum gain were found to be reduced with respect to Lambertian light sources, thus

requiring higher levels of incident X-ray flux to obtain a given level of detector efficiency. It is also of significance to note that the same scintillator host material doped with different activators may exhibit different angular distribution curves. This happens because the type of activator affects the emission spectrum characteristics, which in turn may alter the angular distribution shape through a corresponding modification of the light attenuation coefficient.

Acknowledgement

This work was financially supported by the research programme EPEAEK "Archimidis".

Appendix A

A.1. Normalized angular distribution

The optical signal emitted by a scintillator, may be expressed by either the emitted light energy flux Ψ_λ (in $\mathrm{W\,m^{-2}}$) or the emitted light photon flux Φ_λ (photons per unit of area and time) (Kandarakis and Cavouras, 2001):

$$\Psi^e_\lambda = \int_0^{E_{\max}} \bar{\psi}_x(E)\bar{\eta}(E,t)\eta_C \times \int_0^T x_R(E,t)G_\lambda(\sigma,t)\,\mathrm{d}t\,\mathrm{d}E, \quad (A.1)$$

$$\Phi^e_\lambda = \int_0^{E_{\max}} \bar{\phi}_x(E)\bar{\eta}(E,t)\eta_C n(E,\lambda) \times \int_0^T x_R(E,t)G_\lambda(\sigma,t)\,\mathrm{d}t\,\mathrm{d}E, \quad (A.2)$$

where $\bar{\psi}_x(E)$ is the X-ray energy spectral density distribution $[\mathrm{d}\Psi_x(E)/\mathrm{d}E]$ of the incident X-ray beam, while $\bar{\phi}_x(E)$ is the X-ray photon spectral density distribution $[\mathrm{d}\Phi_x(E)/\mathrm{d}E]$ (Storm, 1972; Tucker et al., 1991). The conversion from $\Phi_x(E)$ into $\Psi_x(E)$, and vice versa, may be obtained by the conversion formula $\Psi_x(E) = \Phi_x(E) \times E$ (Greening, 1985). $n(E,\lambda) = E/E_\lambda$, where E_λ is the mean energy of the emitted light photons and E is the energy of X-ray photons. This factor expresses the number of light photons generated per incident X-ray photon in an ideal scintillator and is used to convert the intrinsic conversion efficiency (η_C) into number of light photons per absorbed X-ray. The second integral in relations (A.1) and (A.2) expresses the light transmission efficiency. The function x_R gives the relative probability of X-ray absorption at depth t, expressed by the relation

$$x_R(E,t)\,\mathrm{d}t = \frac{\mu(E)\,\exp[-\mu(E)t]\,\mathrm{d}t}{\int_0^{wO}\mu(E)\,\exp[-\mu(E)t]\,\mathrm{d}t}, \quad (A.3)$$

where $\mu(E)$ represents the total mass energy absorption coefficient of the scintillator material. The numerator gives the probability for an X-ray photon to be absorbed at depth t within the scintillator and the denominator gives the total probability of X-ray absorption within the whole scintillating screen.

The function G_λ, gives the fraction of light photons, created within an elementary thin layer at depth t, that escape from screen surface. This function was modeled by considering exponential light attenuation determined by the light attenuation coefficient σ (relations (A.1), (A.2)) described in previous studies (Ludwig, 1971; Swank, 1973; Kandarakis and Cavouras, 2001; Kandarakis et al., 2003).

The energy luminous intensity (light energy flux per solid angle element), emitted within a solid angle element $\mathrm{d}\Omega$, is given by the relation

$$I^e(\vartheta) = \frac{1}{4\pi}\int_0^{E_{\max}} \bar{\psi}_x(E)\bar{\eta}(E,t)\eta_C\cos\vartheta \times \int_0^T x_R(E,t)G_\lambda(\vartheta,\sigma,t)\,\mathrm{d}t\,\mathrm{d}E. \quad (A.4)$$

This quantity normalized to zero-degree angle is written as follows:

$$I^e_N(\vartheta) = \frac{\int_0^{E_{\max}} \bar{\psi}_x(E)\bar{\eta}(E,t)\eta_C\cos\vartheta\int_0^T x_R(E,t)G_\lambda(\vartheta,\sigma,t)\,\mathrm{d}t\,\mathrm{d}E}{\int_0^{E_{\max}} \bar{\psi}_x(E)\bar{\eta}(E,t)\eta_C\int_0^T x_R(E,t)G_\lambda(\vartheta=0,\sigma,t)\,\mathrm{d}t\,\mathrm{d}E}. \quad (A.5)$$

The non-normalized photon luminous intensity (light photon flux per unit of solid angle element) is as follows:

$$I^e(\vartheta) = \frac{1}{4\pi}\int_0^{E_{\max}} \bar{\phi}_x(E)\bar{\eta}(E,t)\eta_C n(E,\lambda)\cos\vartheta\int_0^T x_R(E,t)G_\lambda(\vartheta,\sigma,t)\,\mathrm{d}t\,\mathrm{d}E. \quad (A.6)$$

The photon luminous intensity, normalized to zero-degree, is then given as

$$I^e_N(\vartheta) = \frac{\int_0^{E_{\max}} \bar{\phi}_x(E)\bar{\eta}(E,t)\eta_C n(\lambda,E)\cos\vartheta\int_0^T x_R(E,t)G_\lambda(\vartheta,\sigma,t)\,\mathrm{d}t\,\mathrm{d}E}{\int_0^{E_{\max}} \bar{\phi}_x(E)\bar{\eta}(E,t)\eta_C n(\lambda,E)\int_0^T x_R(E,t)G_\lambda(\vartheta=0,\sigma,t)\,\mathrm{d}t\,\mathrm{d}E}. \quad (A.7)$$

A.2. Theoretical model for generation and absorption of K-fluorescence X-rays

The probability of K-fluorescence photon production per absorbed primary X-ray is given as (Chan and Doi, 1983)

$$p_{K\tau}(E) = \frac{w_Z[\mu_p(Z,E)/\rho]}{[\mu_T(E)/\rho]} f_K\omega_K I_y, \quad (A.8)$$

where w_z is the fractional weight of the higher atomic number (Z) element in the scintillator (Gd,Y,Cd, etc), which exhibits the higher probability for photoelectric interaction. $[\mu_P(Z,E)/\rho]$ is the total mass photoelectric X-ray attenuation coefficient of the higher Z element at energy E. $[\mu_T(E)/\rho]$ is the total X-ray mass attenuation coefficient of the scintillator material at energy E. f_K is a factor expressing the relative contribution of the K-shell photoelectric cross section (τ_K) to the total photoelectric effect cross section τ_0 ($f_K = \tau_K/\tau_0$). ω_K is

the K-fluorescence yield of the higher atomic number (Z) element within the scintillator. ω_K expresses the ratio of the average number of K-fluorescence X-rays produced over the number of vacancies created in the K-shell (Auger electrons excluded). I_y is the relative frequency of either K_α or K_β fluorescence X-ray photon production The index y stands either for a K_α or a K_β X-ray fluorescent photon (Storm and Israel, 1967; Chan and Doi, 1983).

The probability, p^t_{Fy}, of generating a K-fluorescence photon within the scintillator layer at depth t (or the tth thin layer), after the incidence of an X-ray photon of energy E, may then be written as follows (Chan and Doi, 1983; Kandarakis et al., 2003):

$$p^t_{Fy}(E) = \frac{w_Z[\mu_p(Z,E)/\rho]}{[\mu_T(E)/\rho]} f_K \omega_K I_y \times \left\{ \exp\left[-\frac{\mu_T(E)}{\rho}(t-1)\Delta t\right] - \exp\left[-\frac{\mu_T(E)}{\rho} t\Delta t\right]\right\}. \quad (A.9)$$

The factor in curly brackets gives the attenuation of incident X-rays within the scintillator layer at depth t (tth layer). Then the probability, p^w_{Fy}, of generating a K-characteristic fluorescence photon within the whole scintillator per incident X-ray photon, may be calculated by the sum

$$p^T_{Fy}(E_y, E) = \sum_{t=1}^{T} p^t_{Fy}(E). \quad (A.10)$$

The probability corresponding to a K-fluorescence X-ray photon, which is generated at depth t (tth scintillator layer), emitted within a solid-angle element $\Delta\Omega_j$, and interacting at depth e (eth layer), may be written as

$$p^{t,e}_{A,j}(E_y, \Delta\Omega_j) = \frac{\Delta\Omega_j}{4\pi}\left\{ \exp\left[-\frac{[\mu_T(E_y)/\rho](|e-t|-1)\rho_p\Delta t}{|\cos(j-1/2)\Delta\xi|}\right] - \exp\left[-\frac{[\mu_T(E_y)/\rho](|e-t|)\rho_p\Delta t}{|\cos(j-1/2)\Delta\xi|}\right]\right\}, \quad (A.11)$$

where $\Delta\Omega_j$ is the solid-angle element subtended at the point of generation of a K-characteristic X-ray fluorescence photon. $\Delta\xi_j$ is the polar angle element corresponding to the solid angle element $\Delta\Omega_j$. r is the radius of a sphere centered at the point of emission. The factor in curly brackets in (7) expresses the interaction of K-fluorescence photons within the eth layer.

The probability of generation and absorption of a K-characteristic fluorescence photon, within the whole scintillator, may be obtained after summation over all the elementary thin layers i and e and over the solid angle elements j, as follows:

$$p^T_{A,F}(E_y, E) = \sum_{t=1}^{T} p^t_{Fy}(E) \sum_{e=1}^{T}\sum_{j=1}^{J} p^{t,e}_{A,j}(E_y, \Delta\Omega_j). \quad (A.12)$$

References

Alig, R.C., Bloom, S., 1977. Cathodoluminescent efficiency. J. Electrochem. Soc. 124, 1136–1138.

Begunov, B.N., Zakaznov, N.P., Kiryushin, S.I., Kuzichev, V.I., 1988. Optical Instrumentation. Theory and Design. Mir Publishers, Moscow, pp. 112–128.

Besch, H.J., 1998. Radiation detectors in medical and biological applications. Nucl. Instr. Methods Phys. Res. A 419, 201–216.

Beutel, J., Mickewich, D.J., Issler, S.L., Shaw, R., 1993. The image quality characteristics of a novel ultra-resolution film/screen system. Phys. Med. Biol. 38, 1195–1206.

Blasse, G., 1994. The luminescence efficiency of scintillators for several applications: state-of-the-art. J. Lumin. 60&61, 930–935.

Cavouras, D., Kandarakis, I., Kannelopoulos, M., Nomicos, C.D., Panayiotakis, G.S., 1999. Signal-to-noise-ratio (SNR) of X-ray imaging scintillators determined by luminescence measurements. Appl. Radiat. Isot. 51, 59–68.

Chan, H.P., Doi, K., 1983. Energy and angular dependence of X-ray absorption and its effect on radiographic response in screen-film systems. Phys. Med. Biol. 28 (5), 565–579.

Curry, T.S., Dowdey, J.E., Murry, R.C., 1990. Luminescent screens. In: Lea, F. (Eds.), Cristensen's Physics of Diagnostic Radiology. London, pp. 118–136.

Diakides, N.A., 1973. Phosphors. Proc. SPIE 42, 83–91.

Giakoumakis, G.E., Miliotis, D.M., 1985. Light angular distribution of fluorescent screens excited by X-rays. Phys. Med. Biol. 30, 21–29.

Giakoumakis, G., Nomicos, C., 1985. Light angular distribution of non-granular fluorescent screens excited by X-rays. Phys. Med. Biol. 30, 993–1003.

Greening, J.R., 1985. Fundamentals of Radiation Dosimetry. Medical Physics Handbooks. Institute of Physics, London.

Haak, G.M., Christensen, N.L., Hammer, B.E., 1997. Experimental studies on the angular distribution of scintillation light from small BGO crystals. Nucl. Instr. Methods Phys. Res. A 390, 191–197.

Hell, E., Knüpfer, W., Mattern, D., 2000. The evolution of scintillating medical detectors. Nucl. Instr. Methods Phys. Res. A 454, 40–48.

Hubbell, J.H., Seltzer, S.M., 1995. Tables of X-ray mass attenuation coefficients and mass energy absorption coefficients 1 keV–20 MeV for elements $Z = 1-92$ and 48 additional substances of dosimetric interest. US Department of Commerce, NISTIR 5632.

Hubbell, J.H., Trehan, P.N., Singh, N., Chand, B., Mehta, D., Garg, M.L., Garg, R.R., Singh, S., Puri, S., 1997. A review, bibliography, and tabulation of K,L and higher atomic shell X-ray fluorescence yields. J. Phys. Chem. Ref. Data. 23 (2), 339–364.

Kandarakis, I., Cavouras, D., 2001. Role of the activator in the performance of scintillators used in X-ray imaging. Appl. Radiat. Isot. 54, 821–831.

Kandarakis, I., Cavouras, D., Panayiotakis, G., Nomicos, C., 1997. Evaluating X-ray detectors for radiographic applications: a comparison of ZnSCdS:Ag with Gd_2O_2S:Tb and Y_2O_2S:Tb screens. Phys. Med. Biol. 42, 1351–1373.

Kandarakis, I., Cavouras, D., Ventouras, E., Nomicos, C., 2003. Theoretical evaluation of granular scintillators quantum gain incorporating the effect of K-fluorescence emission into the energy range from 25 to 100 keV. Radiat. Phys. Chem. 66, 257–267.

Kandarakis, I., Cavouras, D., Nikolopoulos, D., Anastasiou, A., Kalivas, N., Ventouras, E., Dimitropoulos, N., Kalatzis, I., Nomicos, C., Panayiotakis, G., 2005. Evaluation of ZnS: Cu phosphor as X-ray to light converter under mammographic conditions. Radiat. Meas. 39, 263–275.

Ludwig, G.W., 1971. X-ray efficiency of powder phosphors. J. Electrochem. Soc. 118, 1152–1159.

Maidment, A.D.A., Yaffe, M.J., 1995. Analysis of signal propagation in optically coupled detectors for digital mammography: I. Phosphor screens. Phys. Med. Biol. 40, 877–889.

Matveev, A.N., 1985. Optics. Mir Publishers, Moscow, pp. 57–69.

Miura, N., 1999. Phosphors for X-ray and ionizing radiation. In: Shionoya, S., Yen, W.M. (Eds.), Phosphor Handbook. CRC Press, Boca Raton, pp. 177–186.

Press, W.H., Flannery, B.P., Teukolsky, S.A., Vetterling, W.T., 1990. Numerical Recipes in C: The Art of Scientific Computing. Cambridge University Press, Cambridge, pp. 540–547.

Storm, E., 1972. Calculated bremstrahlung spectra from thick tungsten targets. Phys. Rev. A 5, 2328–2338.

Storm, E.H., Israel, H., 1967. Photon cross-sections from 0.001 to 100 MeV for elements 1 through 100, Report LA-3753. Los Alamos Scientific Laboratory of the University of California.

Swank, R.K., 1973. Calculation of modulation transfer functions of X-ray fluorescent screens. Appl. Opt. 12 (8), 1865–1870.

Tucker, D.M., Barnes, G.T., Chakraborty, D.B., 1991. Semi-empirical model for generating tungsten target X-ray spectra. Med. Phys. 18, 211.

van de Hulst, H.C., 1957. Light Scattering by Small Particles. Wiley, New York, pp. 103–107.

van Eijk, C.W.E., 2002. Inorganic scintillators in medical imaging. Phys. Med. Biol. 47, R85–R106.

Wieczorek, B.H., 2001. Physical aspects of detector design. Radiat. Meas. 33, 541–545.

Yu, T., Sabol, J.M., Seibert, J.A., Boone, J.M., 1997. Scintillating fiber optic screens: a comparison of MTF, light conversion efficiency, and emission angle with Gd_2O_2S: Tb screens. Med. Phys. 24, 279.

Zalewski, E.F., 1995. Radiometry and photometry. In: Bass, M., et al. (Eds.), Handbook of Optics. Mc Graw-Hill, New York, pp. 24.3–24.51.